Motif-Based Analysis of Effective Connectivity in Brain Networks

J. Meier, M. Märtens, A. Hillebrand, P. Tewarie and P. Van Mieghem

Abstract Network science has widely studied the properties of brain networks. Recent work has observed a global back-to-front pattern of information flow for higher frequency bands in magnetoencephalography data. However, the effective connectivity at a local level remains yet to be analyzed. On a local level, the building blocks of all networks are motifs. In this study, we exploit the measure of dPTE to analyze motifs of the estimated effective connectivity networks. We find that some 3- and 4-motifs, the bidirectional two-hop path and its extended 4-node versions, are significantly overexpressed in the analyzed networks in comparison with random networks. With a recently developed motif-based clustering algorithm we separate the effective connectivity network in two main clusters which reveal its higher-order organization with a strong information flow between posterior hubs and anterior regions.

J. Meier, M. Märtens and P. Van Mieghem
Delft University of Technology, Faculty of Electrical Engineering, Mathematics and Computer Science, P.O Box 5031, 2600 GA Delft, The Netherlands, e-mail: j.m.meier@tudelft.nl, m.maertens@tudelft.nl and p.f.a.vanmieghem@tudelft.nl

A. Hillebrand
Department of Clinical Neurophysiology and Magnetoencephalography Center, Neuroscience Campus Amsterdam, VU University Medical Center, Amsterdam, The Netherlands, e-mail: a.hillebrand@vumc.nl

P. Tewarie
Department of Neurology, VU University Medical Center, Amsterdam, The Netherlands.
Sir Peter Mansfield Imaging Centre, School of Physics and Astronomy, University of Nottingham, University Park, Nottingham, The United Kingdom, e-mail: prejaas.tewarie@nottingham.ac.uk

1 Introduction

Analyzing the brain as a network has lead to new insights in neuroscience both in understanding healthy and abnormal brain function [22]. Recent studies in neuroscience applied the measure of Phase Transfer Entropy (PTE) to construct the effective connectivity network between brain regions and observed a global posterior-anterior pattern in higher frequency bands [10]. However, the effective connectivity at a local level remains yet to be analyzed. In this study, we analyze with PTE the directionality at a local level in the form of network motifs.

Effective connectivity describes the causal effect of one brain region on another region [1, 7]. To calculate this pairwise value between brain regions, the measure of Transfer Entropy (TE) is often applied [19]. The TE from a region X to a region Y quantifies the improvement in predicting the future of time series X if the present value of Y is also included. Recent work has extended this measure to the analysis of phase time series (Phase Transfer Entropy (PTE); [15]). The advantage of phase time series instead of the original time series is the lower computational cost for analyzing their pairwise interactions [18]. When representing brain regions as nodes and assigning PTE values as link weights, one can build the effective connectivity network. A previous study used PTE for magnetoencephalography (MEG) data from healthy controls and discovered a posterior-anterior directionality in the effective connectivity network of all frequency bands except for the *theta* band (where the pattern was opposite) [10]. The emergence of this pattern is still not completely understood. The hypothesis was that this global directionality is caused by different local properties in the effective connectivity network [10].

On a local scale, network motifs are the building blocks of all networks [17]. On top of the micro-structure of nodes and links, network motifs are small subgraphs that form a higher-order organization of the network [4]. Most commonly, network motifs of 3 or 4 nodes are analyzed. Friedman et al. [6] were recently able to identify Alzheimer patients with directed motif analysis in a so-called progression network. Previous work reported that the motif with ID 78 was overexpressed with respect to random networks in the structural brain networks of the cat and the macaque [21] (see Fig. 2 for motif IDs). The same motif has also been perceived as a good identifier for structural hubs [11]. Recently, Battiston et al. analyzed the interdependency between structure and function in the human brain applying a multilayer motif approach [3]. With computational models of neuronal activity, Battaglia and co-authors [2] linked effective connectivity motifs based on TE to underlying structural motifs and suggested that changes in the effective connectivity lead to different global directions of information flow. With similar motivation of linking frequencies of single motifs to global outcomes, Benson et al. [4] exploited this higher-order organization of the network to define a new motif-based clustering algorithm.

The aim of this study is to investigate effective connectivity motifs in empirical data with the measure of PTE. Therefore, we first explain the construction of the effective connectivity network based on the sending and receiving properties of a node. Then, we analyze the significant motifs in this network. Furthermore, we apply the recently developed motif-based clustering algorithm by Benson et al. [4] on the effective connectivity brain network.

2 Methods

This section explains the measure of directed Phase Transfer Entropy (dPTE), the construction of the directed networks, the motif search and our application of the motif-based clustering.

2.1 Directed Phase Transfer Entropy

The effective connectivity network is based on MEG measurements[1] of 67 healthy controls from a preceding study [10]. We focus our analysis on the *alpha2* frequency band (10-13 Hz) because the previous study observed a significant pattern of posterior-anterior information flow for this frequency band. For every region of interest (ROI) X we compute a time series in the form of a phase time series [18]. We denote a possible value of the signal of region X at time t by x_t and abbreviate the probability that the signal of X equals x_t at an arbitrary time point t to $\Pr[X_t = x_t] = \Pr[x_t]$. The information flow between two ROIs or nodes, X and Y, is then quantified by the Phase Transfer Entropy [15]

$$PTE_{XY}(h) = \sum \Pr\left[x_{t+h}, x_t, y_t\right] \times \log\left(\frac{\Pr\left[x_{t+h}|x_t, y_t\right]}{\Pr\left[x_{t+h}|x_t\right]}\right), \tag{1}$$

for a certain time delay h, where the sum runs over all possible values x_t, x_{t+h} and y_t of the signals. The (joint) probabilities are determined over histograms of their occurrences in an epoch [15]. Following Hillebrand et al. [10] we fix h at

$$h = \frac{N_s \cdot N_{ROI}}{N_{\pm}}, \tag{2}$$

[1] The MEG data were recorded using a 306-channel whole-head MEG system (ElektaNeuromag, Oy, Helsinki, Finland) during a no-task, eyes-closed condition for five consecutive minutes. A beamformer approach was adopted to project MEG data from sensor space to source space [9] and the automated anatomical labelling (AAL) atlas was applied to obtain time series for 78 cortical regions of interest (ROIs) [8, 24]. For each subject, we extracted the first 20 artefact-free epochs of 4096 samples (3.2768 s).

where $N_s = 4096$ and $N_{ROI} = 78$ are the number of samples and the number of ROIs, respectively, and $N_{\pm}$ counts the number of sign changes for the phase across time and ROIs.

Motivated by Hillebrand et al. [10], we define the dPTE for nodes X and Y as

$$dPTE_{XY} = \frac{PTE_{XY}}{PTE_{XY} + PTE_{YX}}, \tag{3}$$

which is a measure of the preferred direction of information flow between nodes X and Y. Since the PTE can only take positive values, this definition of dPTE is well-defined and its value ranges from 0 and 1. If the predominant flow of information is from node X to node Y, then $0.5 < dPTE_{XY} < 1$, else $0 < dPTE_{XY} < 0.5$.

2.2 Constructing the Directed Network

The pairwise dPTEs over all ROIs can be interpreted as a weight matrix of a fully connected network. Since the data is from 67 subjects each over $k = 20$ epochs, we have 1340 weighted networks to begin our construction. We apply a procedure to thin out links and induce a directionality per link instead of a weight. After this transformation, which we call "sparsificiation", we obtain a sparse directed (unweighted) network for each subject, which is amenable for motif search and analysis.

The sparsification (see Fig. 1) contains two steps. First, we discard all links whose weights are in close proximity to 0.5. More precisely, every link whose average weight (over all epochs) is within the closed interval $[0.5 - \alpha\sigma, 0.5 + \alpha\sigma]$ will not be considered, where σ is the standard sample deviation taken over all epochs over all pairs of nodes and α is a positive real control parameter. Under the assumption of a normal distribution with mean 0.5, the 3σ-rule states that this procedure will remove approximately 68% for $\alpha = 1.0$ and 95% for $\alpha = 2.0$ of all links.

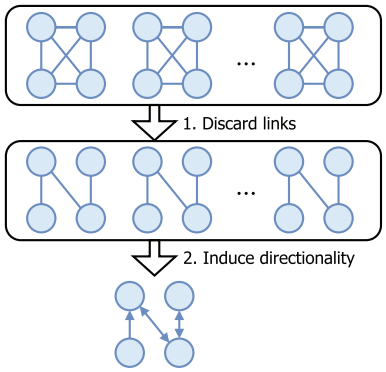

Fig. 1 Schematic overview of the two steps for constructing the directed network (sparsification): (1) discard links close to 0.5 (2) induce directionality for remaining links.

In a second step, we determine for each remaining link whether it should be bi- or uni-directional, and in case of the latter, in which direction the links should be oriented. Clearly, all remaining link weights are now bounded away from 0.5, though it is possible, that for different epochs a single link weight might be lower or higher than 0.5, which makes it ambiguous which member of the node pair is the dominant sender and which the dominant receiver. Let k^+ (k^-) be the number of epochs that the $dPTE_{XY}$ is above (below) 0.5 where $k = k^+ + k^-$ is the total number of epochs for a subject. If $k^+/k \geq 0.75$, we assume X to be a dominant sender and thus we induce a uni-directional link from X to Y. Contrary, we assume X to be a dominant receiver if $k^+/k \leq 0.25$ and point the link from Y to X. If neither applies ($0.25 < k^+/k < 0.75$), we assume that X and Y frequently change roles between dominant sender and dominant receiver. Thus, we induce a bidirectional link between them.

2.3 Motif Search

We are using the excellent *mfinder* software [13], provided by the Uri Alon Lab[2], to search for motifs. We also adopted the motif IDs of mfinder for this work, to be consistent. With sparsification, we generate one directed network for each of the 67 subjects as input for mfinder. Additionally, we construct an averaged effective connectivity network (short: averaged network) by considering all epochs of all subjects together. This construction results in a "virtual" subject with $k = 1340$ instead of $k = 20$ epochs. We set α to 1.0 and 2.0 to compare on different levels of sparsity.

Since the complexity of motif search increases dramatically with the size of the motif, we restrict mfinder to search only for subgraphs of 3 and 4 nodes (further called 3-motifs and 4-motifs). The mfinder program executes two tasks: first, it counts the frequency of all motifs in the original input network. Second, it generates a number of random networks (null model) and determines the motif frequencies in each of them as well. In total, mfinder generates 1000 random networks using the switching algorithm described by Milo et al. [16] for each single input network. We use the default parameters for mfinder, which preserve the degree sequence of the original network and the number of bidirectional links.

A motif is called overexpressed if it occurs significantly more often in the original network than in the random networks. It is essential to keep in mind that a motif which is not overexpressed may still occur quite frequently in the original network, though it arises in a similar frequency by a random link rewiring process. Thus, it can be argued that overexpressed motifs must carry some functional importance for the underlying system since they do not arise merely by chance. We report the motifs that mfinder determines to be overexpressed with z-score > 2.

[2] https://www.weizmann.ac.il/mcb/UriAlon/download/network-motif-software

2.4 Motif-Based Clustering Algorithm

Benson et al. [4] developed a clustering algorithm that partitions a network based on one specific overexpressed motif M. The algorithm constructs clusters by 'cutting' through the minimal possible number of those motifs. Formally, the clustering minimizes the motif conductance defined as

$$\phi_M(S) = \frac{\mathrm{cut}_M(S, S^c)}{\min[\mathrm{vol}_M(S), \mathrm{vol}_M(S^c)]}, \tag{4}$$

where S is the set of nodes in the cluster and S^c its complement. Here, $\mathrm{cut}_M(S, S^c)$ is the number of M motifs that is cut through and $\mathrm{vol}_M(S)$ the number of M motifs that is completely in S. The algorithm can be regarded as an extension of the classic spectral clustering algorithm [25]. The obtained clusters reveal a higher-order organization of the network based on the specific motif M. An implementation of the motif-based clustering algorithm was released as part of the open SNAP framework [14], which we applied to the averaged network using default parameters.

3 Results

We present results for the motif search on 3 and 4 nodes for the individual subjects and for the averaged network, respectively. In addition, we show the results of the motif-based clustering algorithm on the averaged network.

3.1 Significant 3-Motifs

For both variants of the sparsification method ($\alpha = 1$ and $\alpha = 2$), we find the same significant 3-motifs over all subjects meaning that those motifs are more frequent in our analyzed networks than in the null model (see Fig. 2). Those five motifs are not triangular but include all 3-motifs with two links (except for the 2-hop path motif) (Fig. 2(b)- 2(f)). The absolute frequency of those motifs is displayed as a histogram in Fig. 2(a) for the $\pm\sigma$ and the $\pm 2\sigma$ sparsification, respectively. The analysis on the averaged effective connectivity network confirms the over-representation of the motif with ID 78, the bidirectional 2-hop path(Fig. 2(d)), which is the only significant motif that has been found for different sparsification methods (z-scores: 88.25 for $\pm\sigma$ sparsification and 82.7 for $\pm 2\sigma$ sparsification).

3.2 Significant 4-Motifs

In Fig. 3(a) we present a histogram of all significantly overexpressed 4-motifs with the two different sparsification levels. Twelve 4-motifs were found overexpressed in all 67 subject networks (Fig. 3(a), for a visualization see Figs. 3(b)-3(m)).

Analyzing the averaged network we find 3 significant motifs with the $\pm\sigma$ sparsification method (see Figs. 3(l) - 3(n), z-scores: 203.74 for ID 13260, 111.89 for ID 4382 and 14.85 for ID 4698) and none with the $\pm 2\sigma$ method. The two 4-motifs with number 13260 and 4382, the bidirectional ring and the bidirectional star, respectively, have the highest z-scores in the averaged effective connectivity network and are a subset of the significant 4-motifs found for every individual subject (Figs. 3(l) and 3(m)). The overexpression of those two motifs cannot be explained by the higher number of bidirectional links in the effective connectivity network since the null model contains the same number of bidirectional links.

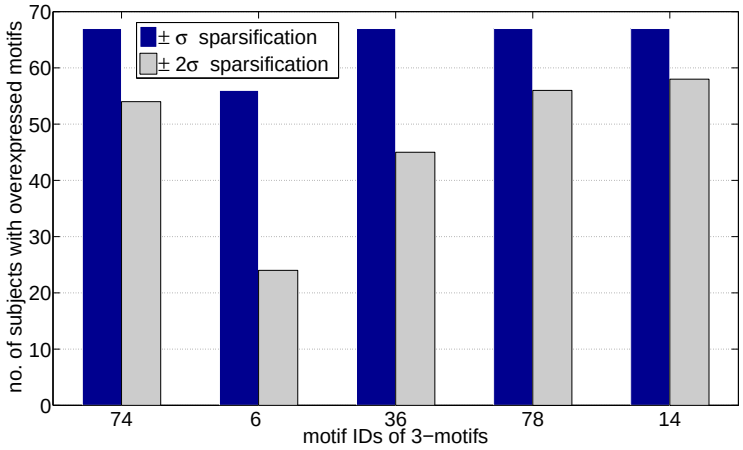

(a) Histogram of all significantly overexpressed 3-motifs.

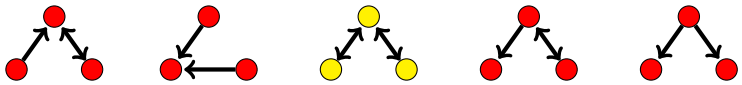

(b) **74** (c) **36** (d) **78** (e) **14** (f) **6**

Fig. 2 **(a)** Frequency of significantly overexpressed 3-motifs over all regarded subjects after the $\pm\sigma$ and $\pm 2\sigma$ sparsification, respectively. **(b)-(f)** All significant 3-motifs over all subjects together with their motif ID. The yellow motif with ID 78 is also overexpressed in the averaged network.

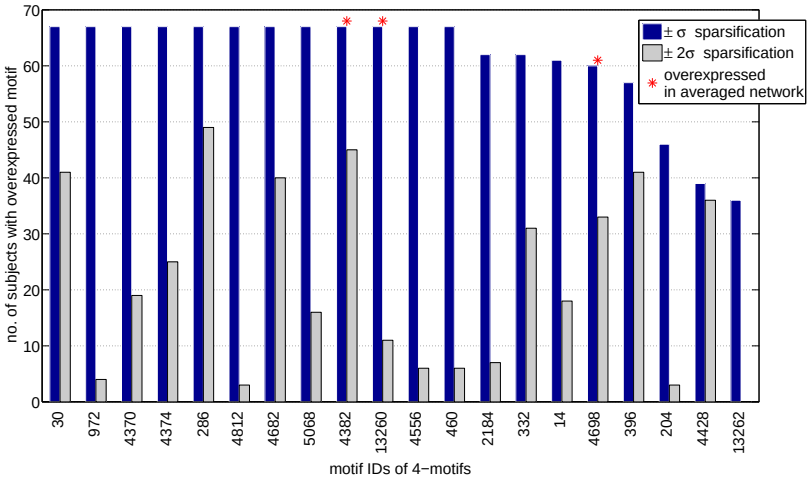

(a) Histogram of the 20 most commonly overexpressed 4-motifs.

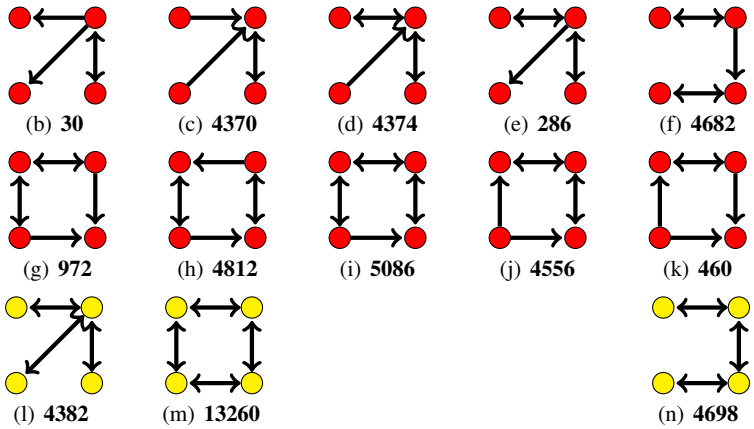

(b) **30** (c) **4370** (d) **4374** (e) **286** (f) **4682**

(g) **972** (h) **4812** (i) **5086** (j) **4556** (k) **460**

(l) **4382** (m) **13260** (n) **4698**

Fig. 3 **(a)** Histogram of the 20 most commonly overexpressed 4-motifs over all subjects after the $\pm\sigma$ and $\pm 2\sigma$ sparsification, respectively. An asterisk marks the motifs that are also overexpressed in the averaged network. **(b)-(m)** The twelve 4-motifs that are overexpressed after the $\pm\sigma$ sparsification in every subject with their motif ID. The yellow motifs are also overexpressed in the averaged network. **(n)** Third overexpressed 4-motif in the averaged network, ID 4698.

3.3 Motif-Based Clusters

Following the approach of [4], we apply the motif-based clustering algorithm on the averaged effective connectivity network. Since for both sparsification methods, the 3-motif with ID 78 was significantly overexpressed in the averaged effective connectivity network and in every subject network, we cluster according to this motif. We find two clusters with the sparsified network for $\pm\sigma$ (Fig. 4). The frontal brain

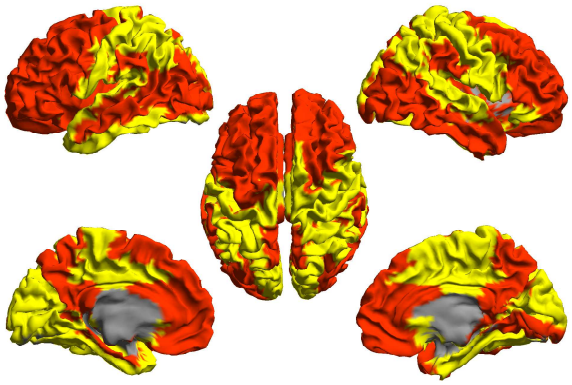

Fig. 4 The two clusters (in red and yellow) on the template brain obtained via the motif-based clustering algorithm after the $\pm\sigma$ sparsification based on the motif 78.

regions seem to be consistently part of the red cluster and the distribution of the clusters across the two brain hemispheres shows a strong symmetry (Fig. 4). The sparser network resulting from the $\pm 2\sigma$ sparsification method was disconnected. Consequently, we could only obtain a motif-based clustering of the largest connected component (see Appendix Fig. 5).

4 Discussion and Conclusions

Evaluating the overexpressed motifs for individual human subjects, it is interesting that the 3-motif with ID 78 and its extended 4-node versions have also been overexpressed in other cortical networks of the cat and the macaque brain [21]. In these motifs some nodes seem highly integrated with their neighbors while others are more segregated. Sporns et al. [21] associated these motifs and the absence of triangular shapes with the general principles of integration and segregation in the functional organization of brain networks. This principle originates from studies of neuronal dynamics where signals from many different spatially segregated groups of neurons are integrated with each other forming one coherent signal [20, 23, 26]. In addition, motif 78 can help to identify hubs in structural brain networks by counting the number of times a node participates in that motif [11]. A possible explanation for this identification is that a hub often connects two otherwise disconnected brain regions reciprocally with each other functioning as a 'bridge' for the information flow [11]. Thus, the pre-dominance of motif 78 in the analyzed effective connectivity network suggests that hubs are 'bridges' for the information flow. The impact on the global network could be further investigated by the new metric of 'bridgeness' [12] in future research. Also the other significant 3-motifs are present in brain networks from the literature. For example, motif 6 has been identified in a previous modeling study with Granger causality as the driving structure behind many neuronal dynamics [5].

The fact that the motif-based clustering reveals a strong symmetry between the brain hemispheres is remarkable and supports the idea of a higher-order organization of the effective connectivity brain network. In comparison, the results of a standard spectral clustering algorithm (edge-based conductance) show a much weaker symmetry and a more disconnected spatial distribution of the two clusters (see Appendix Fig. 6). However, a rather dense network ($\pm\sigma$) seems to be necessary for the emergence of a higher-order structure since the clustering for the sparser averaged network ($\pm 2\sigma$) appears to be frail (see Appendix Fig. 5). Thus, finding an optimal link density for motif-based clustering requires further investigation.

Looking into the obtained clusters, we find that the red cluster in Fig. 4 consists of all frontal brain regions and some posterior regions which are known to be the strongest structural hubs [10]. The fact that the motif-based clustering algorithm does not separate posterior hubs and frontal regions suggests that there might be an increased information flow between them. This result strengthens the hypothesis from [10] that the posterior hubs play a crucial role in the global information flow of the effective connectivity. More specifically, posterior hubs in the brain seem to play the role of a 'bridge' for not only the local but also the global information flow. However, this 'bridge' seems to be active in varying pre-dominant directions for different frequency bands [10]. To conclude, our study shows a promising way of integrating local structures to explain the emergence of global patterns in brain networks. This approach might be a first stepping stone towards understanding the information flow in the healthy brain which could, in the future, support the diagnosis of brain disorders.

Acknowledgements This work was partially supported by a private sponsorship to the VUmc MS center Amsterdam. The VUmc MS center Amsterdam is sponsored through a program grant by the Dutch MS Research Foundation (Grant number 09-358d). We thank Cornelis J. Stam for his useful comments and input that improved the paper. We are grateful to Jure Leskovec, who made his code for the motif-based clustering publicly available as part of the SNAP framework.

Appendix

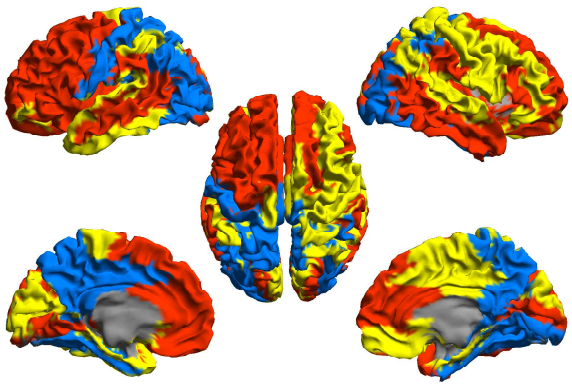

Fig. 5 The two main clusters (in red and yellow) of the largest connected component on the template brain obtained via the motif-based clustering algorithm after the $\pm 2\sigma$ sparsification based on the motif 78. The blue colored regions were not in the largest connected component.

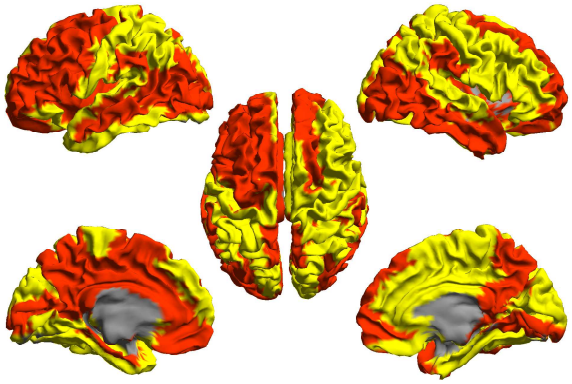

Fig. 6 The two main clusters (in red and yellow) on the template brain obtained via the spectral clustering algorithm with the $\pm\sigma$ sparsification. In comparison with the motif-based clustering in Fig. 4, the red cluster looks more disconnected and does not include all anterior regions anymore.

References

1. Aertsen, A., Gerstein, G., Habib, M., Palm, G.: Dynamics of neuronal firing correlation: modulation of" effective connectivity". Journal of Neurophysiology **61**(5), 900–917 (1989)
2. Battaglia, D., Witt, A., Wolf, F., Geisel, T.: Dynamic effective connectivity of inter-areal brain circuits. PLoS Comput Biol **8**(3), e1002,438 (2012)
3. Battiston, F., Nicosia, V., Chavez, M., Latora, V.: Multilayer motif analysis of brain networks. arXiv preprint arXiv:1606.09115 (2016)
4. Benson, A.R., Gleich, D.F., Leskovec, J.: Higher-order organization of complex networks. Science **353**(6295), 163–166 (2016)

5. Deng, B., Deng, Y., Yu, H., Guo, X., Wang, J.: Dependence of inter-neuronal effective connectivity on synchrony dynamics in neuronal network motifs. Chaos, Solitons & Fractals **82**, 48–59 (2016)
6. Friedman, E.J., Young, K., Tremper, G., Liang, J., Landsberg, A.S., Schuff, N., Initiative, A.D.N., et al.: Directed network motifs in alzheimer's disease and mild cognitive impairment. PloS One **10**(4), e0124,453 (2015)
7. Friston, K.J.: Functional and effective connectivity in neuroimaging: a synthesis. Human Brain Mapping **2**(1-2), 56–78 (1994)
8. Gong, G., He, Y., Concha, L., Lebel, C., Gross, D.W., Evans, A.C., Beaulieu, C.: Mapping anatomical connectivity patterns of human cerebral cortex using in vivo diffusion tensor imaging tractography. Cerebral Cortex **19**(3), 524–536 (2009)
9. Hillebrand, A., Barnes, G.R., Bosboom, J.L., Berendse, H.W., Stam, C.J.: Frequency-dependent functional connectivity within resting-state networks: an atlas-based meg beamformer solution. NeuroImage **59**(4), 3909–3921 (2012)
10. Hillebrand, A., Tewarie, P., van Dellen, E., Yu, M., Carbo, E.W., Douw, L., Gouw, A.A., van Straaten, E.C., Stam, C.J.: Direction of information flow in large-scale resting-state networks is frequency-dependent. Proceedings of the National Academy of Sciences **113**(14), 3867–3872 (2016)
11. Honey, C.J., Kötter, R., Breakspear, M., Sporns, O.: Network structure of cerebral cortex shapes functional connectivity on multiple time scales. Proceedings of the National Academy of Sciences **104**(24), 10,240–10,245 (2007)
12. Jensen, P., Morini, M., Marton, K., Venturini, T., Vespignani, A., Jacomy, M., Cointet, J.P., Merckle, P., Fleury, E.: Detecting global bridges in networks. Journal of Complex Networks **4**, 319–329 (2016)
13. Kashtan, N., Itzkovitz, S., Milo, R., Alon, U.: Mfinder tool guide. Department of Molecular Cell Biology and Computer Science and Applied Mathematics, Weizmann Institute of Science, Rehovot Israel, Tech Rep (2002)
14. Leskovec, J., Sosič, R.: Snap: A general-purpose network analysis and graph-mining library. ACM Transactions on Intelligent Systems and Technology (TIST) **8**(1), 1 (2016)
15. Lobier, M., Siebenhühner, F., Palva, S., Palva, J.M.: Phase transfer entropy: a novel phase-based measure for directed connectivity in networks coupled by oscillatory interactions. NeuroImage **85**, 853–872 (2014)
16. Milo, R., Kashtan, N., Itzkovitz, S., Newman, M.E., Alon, U.: Uniform generation of random graphs with arbitrary degree sequences. arXiv preprint cond-mat/0312028 **106**, 1–4 (2003)
17. Milo, R., Shen-Orr, S., Itzkovitz, S., Kashtan, N., Chklovskii, D., Alon, U.: Network motifs: simple building blocks of complex networks. Science **298**(5594), 824–827 (2002)
18. Rosenblum, M., Pikovsky, A., Kurths, J., Schäfer, C., Tass, P.A.: Phase synchronization: from theory to data analysis. Handbook of Biological Physics **4**, 279–321 (2001)
19. Schreiber, T.: Measuring information transfer. Physical Review Letters **85**(2), 461 (2000)
20. Sporns, O., Chialvo, D.R., Kaiser, M., Hilgetag, C.C.: Organization, development and function of complex brain networks. Trends in Cognitive Sciences **8**(9), 418–425 (2004)
21. Sporns, O., Kötter, R.: Motifs in brain networks. PLoS Biol **2**(11), e369 (2004)
22. Stam, C.J., Van Straaten, E.: The organization of physiological brain networks. Clinical Neurophysiology **123**(6), 1067–1087 (2012)
23. Tononi, G., Edelman, G.M., Sporns, O.: Complexity and coherency: integrating information in the brain. Trends in Cognitive Sciences **2**(12), 474–484 (1998)
24. Tzourio-Mazoyer, N., Landeau, B., Papathanassiou, D., Crivello, F., Etard, O., Delcroix, N., Mazoyer, B., Joliot, M.: Automated anatomical labeling of activations in spm using a macroscopic anatomical parcellation of the mni mri single-subject brain. NeuroImage **15**(1), 273–289 (2002)
25. Van Mieghem, P.: Graph Spectra for Complex Networks. Cambridge University Press (2011)
26. Zhigulin, V.P.: Dynamical motifs: building blocks of complex dynamics in sparsely connected random networks. Physical Review Letters **92**(23), 238,701 (2004)